doi:10.1093/brain/awt095 Brain 2013: 136; 1708–1717 | 1708

BRAIN
A JOURNAL OF NEUROLOGY

Beta-propeller protein-associated neurodegeneration: a new X-linked dominant disorder with brain iron accumulation

Susan J. Hayflick,[1,2,3] Michael C. Kruer,[4] Allison Gregory,[1] Tobias B. Haack,[5,6] Manju A. Kurian,[7,8] Henry H. Houlden,[9] James Anderson,[10] Nathalie Boddaert,[11] Lynn Sanford,[1] Sami I. Harik,[12] Vasuki H. Dandu,[12] Nardo Nardocci,[13] Giovanna Zorzi,[13] Todd Dunaway,[14] Mark Tarnopolsky,[15] Steven Skinner,[16] Kenton R. Holden,[16] Steven Frucht,[17] Era Hanspal,[18] Connie Schrander-Stumpel,[19] Cyril Mignot,[20] Delphine Héron,[20] Dawn E. Saunders,[21] Margaret Kaminska,[22] Jean-Pierre Lin,[22] Karine Lascelles,[22] Stephan M. Cuno,[5,6] Esther Meyer,[7] Barbara Garavaglia,[23] Kailash Bhatia,[24] Rajith de Silva,[25] Sarah Crisp,[25] Peter Lunt,[26] Martyn Carey,[27] John Hardy,[9] Thomas Meitinger,[5,6] Holger Prokisch[5,6] and Penelope Hogarth[1,3]

1 Department of Molecular and Medical Genetics, Oregon Health and Science University, Portland, 97239 USA
2 Department of Paediatrics, Oregon Health and Science University, Portland, 97239 USA
3 Department of Neurology, Oregon Health and Science University, Portland, 97239 USA
4 Sanford Children's Health Research Centre, Sioux Falls, SD 57104 USA and Departments of Paediatrics and Neurosciences, University of South Dakota, Vermillion, SD 57069, USA
5 Institute of Human Genetics, Technische Universität München, 85748 Munich, Germany
6 Institute of Human Genetics, Helmholtz Zentrum München, German Research Centre for Environmental Health, 85764 Neuherberg, Germany
7 Neurosciences Unit, Institute of Child Health, University College London WC1N 3LU, UK
8 Department of Paediatric Neurology, Great Ormond Street Hospital, London WC1N 3JH, UK
9 Department of Molecular Neuroscience and Reta Lilla Weston Laboratories, UCL Institute of Neurology, Queen Square, London WC1N 3BG, UK
10 Department of Radiology, Oregon Health and Science University, Portland, 97239 USA
11 Department of Paediatric Radiology, Hôpital Necker Enfants Malades, 75743 Paris, France
12 Department of Neurology, University of Arkansas for Medical Sciences, Little Rock, AR, 72205 USA
13 Unit of Child Neurology, Department of Paediatric Neuroscience IRCCS Foundation Neurological Institute 'Carlo Besta', 20133 Milan Italy
14 Neurology LLPC, Tulsa OK 74104 USA
15 Division of Neuromuscular and Neurometabolic Disorders, Department of Paediatrics, McMaster University Medical Centre, Hamilton L8N 3Z5 Canada
16 Greenwood Genetic Centre, Greenwood, SC 29646 USA
17 Department of Neurology, Mount Sinai School of Medicine, New York, NY 10029 USA
18 Parkinson's Disease and Movement Disorders Centre, Albany Medical Centre, and Department of Neurology, Albany Medical College, NY 12208 USA
19 Department of Clinical Genetics and School for Oncology and Developmental Biology (GROW), Maastricht UMC+, Maastricht, The Netherlands
20 Clinical Genetics Unit, Centre de Référence des Déficiences Intellectuelles de Causes Rares, Groupe Hospitalier Pitié-Salpêtrière, 75651 Paris, France
21 Department of Paediatric Radiology, Great Ormond Street Hospital, London WC1N 3BG, UK
22 Children's Neurosciences Centre, Evelina Children's Hospital, Guy's and St Thomas' NHS Foundation Trust, London SE1 7EH UK
23 Unit of Molecular Neurogenetics, IRCCS, Foundation Neurological Institute 'Carlo Besta', 20133 Milan, Italy
24 Sobell Department of Motor Neuroscience and Movement Disorders, UCL Institute of Neurology, Queen Square, London WC1N 3BG, UK
25 Department of Neurology, Essex Centre for Neurological Sciences, Queen's Hospital, Romford, Essex RM7 0AG, UK
26 Clinical Genetics Department, University Hospitals Bristol, NHS Foundation Trust, Bristol BS2 8EG, UK
27 Department of Pathology, University Hospitals Birmingham NHS Foundation Trust, Queen Elizabeth Hospital, Birmingham B15 2WB, UK

Received December 3, 2012. Revised February 22, 2013. Accepted February 24, 2013. Advance Access publication May 17, 2013

Correspondence to: Susan Hayflick,
Department of Molecular and Medical Genetics,
Oregon Health and Science University,
Portland,
97239 USA
E-mail: hayflick@ohsu.edu

Neurodegenerative disorders with high iron in the basal ganglia encompass an expanding collection of single gene disorders collectively known as neurodegeneration with brain iron accumulation. These disorders can largely be distinguished from one another by their associated clinical and neuroimaging features. The aim of this study was to define the phenotype that is associated with mutations in *WDR45*, a new causative gene for neurodegeneration with brain iron accumulation located on the X chromosome. The study subjects consisted of *WDR45* mutation-positive individuals identified after screening a large international cohort of patients with idiopathic neurodegeneration with brain iron accumulation. Their records were reviewed, including longitudinal clinical, laboratory and imaging data. Twenty-three mutation-positive subjects were identified (20 females). The natural history of their disease was remarkably uniform: global developmental delay in childhood and further regression in early adulthood with progressive dystonia, parkinsonism and dementia. Common early comorbidities included seizures, spasticity and disordered sleep. The symptoms of parkinsonism improved with L-DOPA; however, nearly all patients experienced early motor fluctuations that quickly progressed to disabling dyskinesias, warranting discontinuation of L-DOPA. Brain magnetic resonance imaging showed iron in the substantia nigra and globus pallidus, with a 'halo' of T_1 hyperintense signal in the substantia nigra. All patients harboured *de novo* mutations in *WDR45*, encoding a beta-propeller protein postulated to play a role in autophagy. Beta-propeller protein-associated neurodegeneration, the only X-linked disorder of neurodegeneration with brain iron accumulation, is associated with *de novo* mutations in *WDR45* and is recognizable by a unique combination of clinical, natural history and neuroimaging features.

Keywords: iron; NBIA; autophagy; basal ganglia; Rett syndrome

Abbreviation: BPAN = beta-propeller protein-associated neurodegeneration; NBIA = neurodegeneration with brain iron accumulation

Introduction

Neurodegeneration with brain iron accumulation (NBIA) encompasses a group of single gene disorders that share the feature of high brain iron. Causative genes have been identified for most patients with NBIA; however, the genetic basis remains to be found for ~35% of them (Hogarth *et al.*, 2013). Recently, a new NBIA gene was identified on the X chromosome (Haack *et al.*, 2012). As with other new disease gene discoveries, we sought to delineate the phenotype associated with mutations in this gene, *WDR45*, in an attempt to assist clinicians with the diagnostic evaluation.

WDR45 encodes a protein that serves a putative role in autophagy, a lysosomal process to degrade cellular components that is thought to be defective in many neurodegenerative disorders (Behrends *et al.*, 2010). The protein encoded by WDR45 belongs to a family that includes LIS1 (now known as PAFAH1B1), which is defective in lissencephaly, along with other proteins important for neuronal survival. This protein is characterized as a beta-propeller scaffold that serves as a platform to enable specific protein–protein interactions that are important in autophagy. Although the precise mechanism by which defective WDR45 causes disease is unknown, a clear pattern of clinical, imaging and natural history data enables the recognition of this distinctive phenotype and the ascertainment of patients. This NBIA disorder was called 'beta-propeller protein-associated neurodegeneration' (BPAN) (Haack *et al.*, 2012). Studies of patients with BPAN will help to advance understanding of disease pathogenesis and may yield new insights into more common neurodegenerative disorders such as Rett syndrome, the epileptic encephalopathies and Parkinson's disease.

Materials and methods

Subjects

We recruited subjects into an NBIA research repository that includes clinical data and associated DNA samples. Subjects were recruited through a research listing on GeneTests, the Oregon Health and Science University website, and at NBIA Disorders Association international family conferences. Samples from 14 individuals with idiopathic NBIA who shared a distinctive phenotype of early developmental delay with regression and parkinsonism in adulthood were investigated using whole exome sequencing techniques and have been included in an earlier report (Haack *et al.*, 2012). Patients found to harbour a mutation in *WDR45* were included in further analyses. The cohort of subjects sent for whole exome sequencing were all determined to have NBIA based on MRI evidence of high iron in the basal ganglia, as well as accompanying neurological signs and symptoms. All had previously been screened for mutations in known NBIA genes (*PANK2*, *PLA2G6*, *C19orf12*, *FA2H*). The subjects, although ethnically diverse, were clinically and radiographically homogeneous.

We subsequently screened for mutations in selected samples from the Oregon Health and Science University NBIA cohort and from four large international idiopathic NBIA cohorts (~60 individual samples) collected through the Neurosciences Unit at the Institute of Child Health (University College London), the National Hospital for Neurology and Neurosurgery (UK), the Institute of Human Genetics, Technische Universität München (Germany), and the Unit of Molecular Neurogenetics, IRCCS, Foundation Neurological Institute 'Carlo Besta' (Italy).

Direct examinations were completed on 11 subjects, three males and eight females, and medical records were reviewed on all 23 patients included in this report. Only partial clinical data were available on some patients.

Analysis of mutations

We used primer sets to amplify all *WDR45* exons and adjacent intronic sequences, including splice signals, and sequenced DNA from the affected individual in each family as well as their parents and siblings, when available. We analysed sequence variants that did not cause a frameshift or stop codon using SIFT, PolyPhen2, PMut, and PhD-SNP algorithms to predict pathogenicity (Ng, 2003; Ferrer-Costa, 2005; Capriotti, 2006; Adzhubei *et al.*, 2010).

Standard protocol approvals, registrations and patient consents

DNA and clinical information were collected and used after participants had given written informed consent according to the protocol approved by the institutional review boards.

Results

Twenty-three subjects were found to be *WDR45* mutation-positive. No mutations were detected in parents or siblings who were tested. In 13 patients, pathogenic mutations were first identified in *WDR45* by whole exome sequencing and then confirmed by direct sequencing of the gene. Subsequent screening of patients with idiopathic NBIA led to the identification of 10 additional subjects with deleterious mutations in *WDR45*. Loss-of-function mutations accounted for the variants found in 20 subjects. Three missense mutations were identified in highly conserved residues and were predicted to be deleterious (Haack *et al.*, 2012).

All subjects had been diagnosed with global developmental delay in infancy or early childhood and carried a diagnosis of intellectual disability into adulthood. Most children made slow developmental gains over time. Developmental quotients ranged from 30–50, with severely limited expressive language in childhood. As children, most subjects were described as clumsy with a broad-based or ataxic gait but were generally healthy. Six were noted to have spasticity. Thirteen subjects had epilepsy in childhood requiring treatment with anti-epileptic medication. Various seizure types were reported in these patients, including focal seizures with altered levels of consciousness, absence seizures, atonic seizures with head nodding, generalized seizures with fever, epileptic spasms, generalized tonic-clonic seizures, and myoclonic seizures. Multiple seizure types were prevalent in some individuals. EEG changes that were reported included spike and slow wave activity; focal/generalized epileptiform discharges; and diffuse background slowing with superimposed bursts of fast rhythms. Table 1 provides a detailed summary of each subject's clinical, radiographic and genetic features.

All subjects exhibited neurological deterioration in adolescence or early adulthood with the onset of dystonia, parkinsonism, and new cognitive decline. The mean age at deterioration was 25.3 years (range 15–37 years). The parkinsonism was characterized by prominent bradykinesia, rigidity and freezing of gait; however, tremor was noted in only two subjects. Dystonia was a common feature beginning in adolescence or early adulthood, typically starting in the upper extremities. One subject was described with a dystonic 'bent trunk' gait suggestive of camptocormia. Subjects treated with L-DOPA had striking benefit from the drug, with improved motor function, affect, appetite and interest in activities. Equally consistently, the duration of L-DOPA benefit was relatively short, with early appearance of motor fluctuations quickly advancing to disabling dyskinesias and requiring discontinuation of drug within a few years. Dopaminergic agonists were tried in at least two patients but dyskinesias limited their use. Patients were documented to have deterioration of cognition concomitant with onset of the movement disorder, with progressive loss of limited expressive language skills advancing to severe dementia in end stages. Eighteen subjects are living, and their current ages range from 16 to 44 years. Five female subjects died during their third to fifth decades of life; one died with severe parkinsonism and dysphagia at 48 years of age, which was 11 years after her neurological deterioration reportedly began. Two died from aspiration pneumonia, and two died from unknown causes.

Additional phenotypic features reported in only a subset of patients included disordered sleep, ocular defects and Rett-like hand stereotypies (Table 1). Interestingly, sleep abnormalities were specifically noted in six subjects and included a positive multiple sleep latency test with shortened mean sleep latency and abnormal REM sleep (documented at age 5 years), hypersomnolence, hyposomnolence, and 'dance-like' movements of extremities with onset of sleep. Seven subjects were reported to have ocular defects, including patchy loss of the pupillary ruff (also seen in pantothenate kinase-associated neurodegeneration) (Egan *et al.*, 2005), bilateral partial retinal colobomata, high myopia, astigmatism with myopia, and spontaneous retinal detachment. Seven females were suspected to have atypical Rett syndrome, two of whom had repetitive midline hand-wringing behaviour. By early adulthood, bowel and bladder incontinence were manifest in most subjects with BPAN. The basis for this is unclear.

With neurological deterioration in adolescence or adulthood, all subjects underwent brain MRI, revealing a strikingly consistent pattern of abnormalities. All MRIs were reported to show evidence of increased iron in the substantia nigra and globus pallidus. Thirteen MRIs from 11 subjects were available to us for review. All MRIs showed T_2 hypointense signal in the substantia nigra and globus pallidus (Fig. 1). Consistently, the substantia nigra abnormal signal, which included the cerebral peduncles, was more hypointense than that of the globus pallidus. There was a variable degree of globus pallidus hypointensity on T_2-weighted images (6 of 10 subjects) with the strongest signal localizing to a

Table 1 Clinical, radiographic and genetic features of BPAN

Subject ID	Gender	Age (years)	Age at deterioration (Years)	Complementary DNA (NM_007075.3)	Protein (NP_009006)	Developmental delay with intellectual disability	Progressive psychomotor slowing adolescence/ adulthood	Rett-like features	Dystonia	Parkinsonism	L-DOPA responsive	Limited expressive language	Sleep problems	Epilepsy	Ocular defects	T_2 hypointense substantia nigra and globus pallidus (high iron)	T_1 hyperintense 'halo' midbrain	Cerebral atrophy	Cerebellar atrophy	Other features
60251[P]	F	23	–	c.1007_1008del[^]	p.Tyr336Cysfs*5	+	+	repetitive midline handwringing	+	+	unk	+	REM sleep disorder	+[1,2]	Astigmatism, myopia	+	+	+	–	
63700[P]	F	44	26	c.38G>C[^]	p.Arg13Pro	+	+	–	+	+	+	+	–	–	–	+	+	–		
63701[P]	F	30	26	c.-1_5del	p.Met1?	+	+	+	+	+	+	+	Excessive movement during sleep	+[2]	High myopia, abnormal pupil shape	+	+	+	–	
63702[P]	F	29	–	c.293T>C	p.Leu98Pro	+	+	–	+	–	na	+	–	+[2]	–	+	+	+	–	Posterior ventriculomegaly
63703[P]	F	43	26	c.476del	p.Leu159Argfs*2	+	+	–	+	+	unk	+	Sleep-wake cycle disorder	–	–	+	+	+	–	
63704[P]	F	34	25	c.19C>T	p.Arg7*	+	+	–	+	+	+	+	–	–	Spontaneous retinal detachment	+	+	+		
63705[P]	F	22	15	c.56-1G>A	splicing defect	+	+	Hand sterotypies	+	+	unk	+	–	+[1,3]	Bilateral partial retinal coloboma	+	+	–	–	
63706[P]	F	39♀	29	c.700C>T	p.Arg234*	+	+	–	+	+	+	+	–	+[2,3]	–	+	+	–		Stroke
63707[P]	F	49♀	37	c.400C>T[^]	p.Arg134*	+	+	–	+	+	+	+	Hypersomnolence with choreiform movements at onset of sleep	+[3]	–	+	+	+	–	
63708[P]	M	37	27	c.228_229del[^]	p.Glu76Aspfs*38	+	+	–	+	+	+	+	–	–	–	+	+	+	–	Mega cisterna magna; stroke
63709[P]	F	40	30	c.405_409del	p.Lys135Asnfs*2	+	+	–	+	+	+	+	–	–	Patchy loss of pupillary ruff	+	+	+	+	
63711[P]	F	45♀	31	c.359dup[^]	p.Lys121Glufs*18	+	+	–	+	+	unk	+	–	–	–	+	+	+		
63712[P]	F	37	26	c.830+1G>A[^]	splicing defect	+	+	+	+	+	unk	+	Parasomnia with nocturnal screaming	–	–	+	+	+	+	
49841[P]	M	31	28	c.19dup	p.Arg7Profs*64	+	+	–	+	+	na	+	+	+[3]	VEP: increased latency	+	–	+	–	
HS411-201[P]	F	35	30	c.235+1G>A[^]	splicing defect	+	+	–	+	+	unk	+	–	–	–	+	+	+	+	
HH56[P]	F	24	19	c.1007_1008del[^]	p.Tyr336Cysfs*5	+	+	–	+	+	unk	+	–	+[4]	–	+	+	+	–	
HH84[P]	F	44♀	unk	c.694_703del[^]	p.Leu232Alafs*53	+	+	–	+	+	+	+	–	–	–	+	+	+	–	Uterine tumour
NBIA10[P]	F	17	16	c.183C>A[^]	p.Asn61Lys	+	+	–	+	+[5]	+	+	–	+[2]	–	+	+	–	+	
HS463[P]	M	31	26	c.1025_1034del insACATATTT	p.Gly342Aspfs*12	+	+	–	+	+	+	+	–	+[2]	–	+	+	+	–	
HS152[P]	F	43	25	c.55+1G>C[^]	splicing defect	+	+	+	+	+	+	+	–	+[1,2]	–	+	+	+	–	
NBIA18	F	27♀	20	c.830 + 2T>C[^]	splicing defect	+	+	–	+	+	unk	+	–	–	–	unk	unk	+	–	Neuropathology
NBIA21	F	31	29	c.1A>G	start codon abolished	+	+	+	+	–	na	+	–	+[3]	–	+	+	+	+	
HS415	F	16	15	c.186delT	p.Leu63Trp fs*19	+	+	+	+	+[6]	unk	+	–	+[2]	High myopia	+	–	+	+	

♀Deceased.
[^]Confirmed *de novo* mutation.
[P]Reported in a previous publication Haack *et al.* 2012.
na = not applicable.
unk = unknown.
[1]EEG: diffuse background slowing with bursts of generalized 3/s spike and wave discharges.
[2]Staring, absence or atonic seizures.
[3]Febrile seizures.
[4]Myoclonic seizures.
[5]Minimal parkinsonism only: freezing of gait, hesitancy at doorways.
[6]Minimal parkinsonism only: rigidity.
VEP = visual evoked potential.

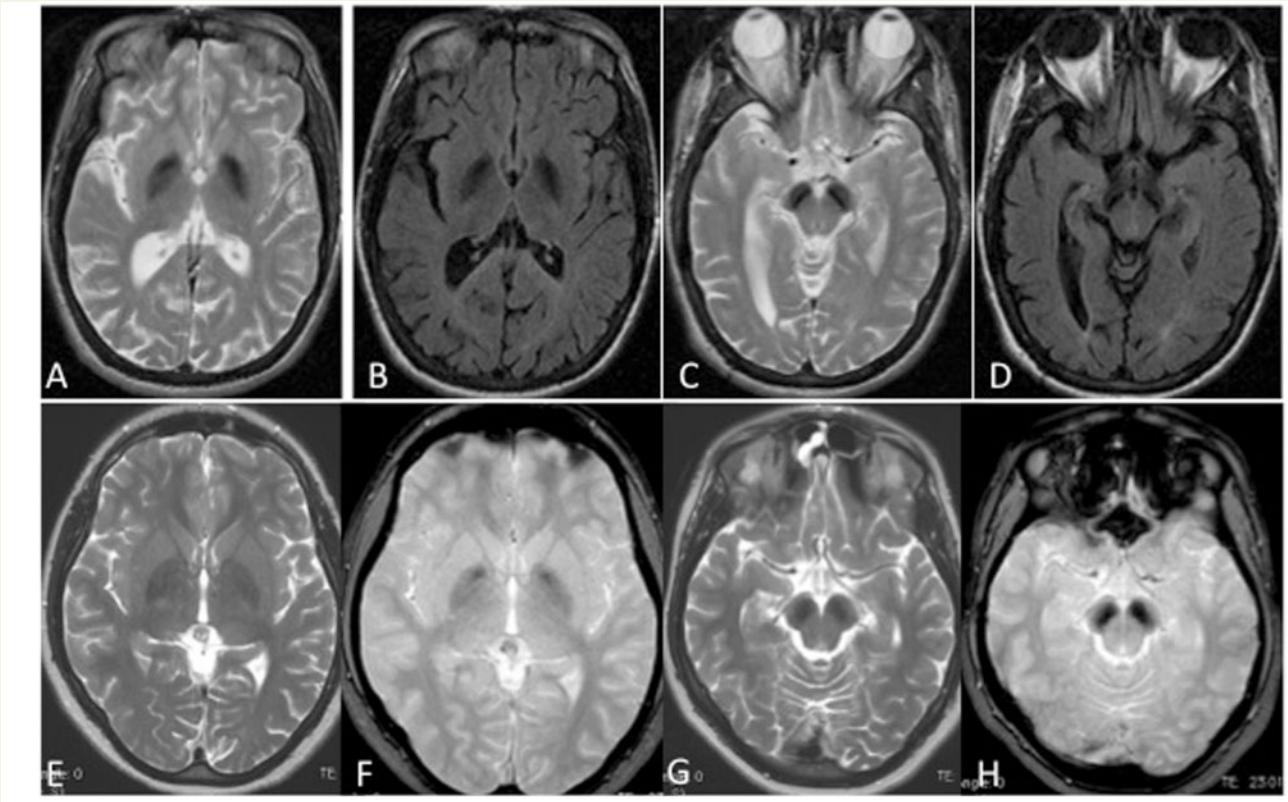

Figure 1 MRI showing iron in BPAN. The globus pallidus is variably hypointense on axial T_2 (**A** and **E**) and more so on FLAIR sequence (**B**) and T_2^* sequence (**F**). Substantia nigra (T_2, **C** and **G**; FLAIR, **D**; T_2^*, **H**) shows even greater hypointensity, indicating high levels of iron in these structures.

more anterior and central focus within the globus pallidus interna (Fig. 1).

On T_1-weighted axial imaging, the substantia nigra and cerebral peduncles demonstrated a thin, dark central band surrounded by a halo of hyperintense signal in 8 of 10 subjects using 1.5 T scanners (Fig. 2). Only sagittal views were available on the two patients, and both showed T_1 hyperintensity in the substantia nigra. In the three patients studied on a 3.0 T field strength scanner, this feature was less striking but still visible (Fig. 2). Whether this is due to a difference in field strength or subject variability is uncertain.

Generalized cerebral atrophy was observed in 19 of 23 subjects, with primarily supratentorial volume loss and some involvement of mid-brain. Volume loss was greater in those with more advanced disease. Cerebellar atrophy was observed in six subjects.

Other MRI changes less consistently seen in adults included subtle T_2 hypointensity in the area lying between the transverse level of the substantia nigra and the globus pallidus, thinning of the corpus callosum, and possible increases in signal intensity in the periaqueductal grey matter. Two patients demonstrated T_1 mildly hyperintense signal in the globus pallidus. Scattered T_2 white matter hyperintensities were observed in two subjects. A CT scan was available on only one subject and showed hyperdensity in the substantia nigra, which would be consistent with iron.

Interestingly in our youngest patients imaged following neurological deterioration (MRIs done at ages 15 and 16 years), the T_1 hyperintense signal in substantia nigra was much less prominent than in the older age group, but the T_2 hypointense signal in substantia nigra was still quite prominent (Fig. 3). Similar changes were seen with T_2^* sequence, whereas FLAIR tended to highlight changes that were less evident on T_2 (Fig. 3).

In contrast to the markedly abnormal neuroimaging seen in adulthood, scans obtained during early childhood were nearly all reported as normal. A brain MRI done at 14 months of age for developmental delay was reviewed and was normal. CT scans in three subjects done during childhood were reported to be normal, and two were reported to show atrophy.

Neuropathological features of BPAN are shown in Fig. 5, from a female who died from pneumonia at 27 years of age (Patient NBIA-18). The gross findings included mild cerebellar atrophy, thinned cerebral peduncles and dark grey-brown appearance of substantia nigra and, to a much lesser extent, globus pallidus. On microscopic examination, the globus pallidus and substantia nigra stained strongly for iron and demonstrated numerous large axonal spheroids, siderophages, reactive astrocytes and severe neuronal loss. Axonal spheroids were seen also in pons, medulla and thalamus but were fewer in number. The putamen and thalamus showed gliosis and mild neuronal loss. Significant loss of Purkinje cells and axonal 'torpedoes' was evident in the granular cell layer. Numerous tau-positive neurofibrillary tangles were seen in hippocampus, neocortex, putamen, and hypothalamus, with

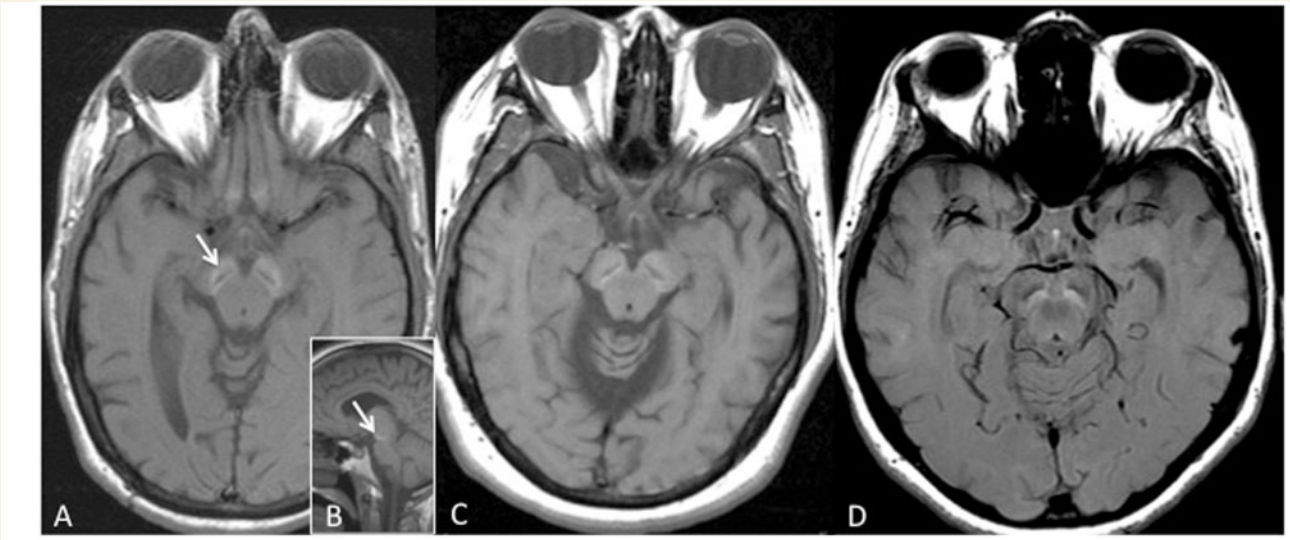

Figure 2 The halo in the substantia nigra is unique to BPAN. On T_1-weighted axial imaging, substantia nigra shows a halo of hyperintense signal surrounding a thin linear region of hypointense signal on 1.5 T (**A** and sagittal view in **B** and **C**) and 3.0 T (**D**) field strength scanners.

fewer seen in remaining neurons in globus pallidus, substantia nigra, pons and thalamus. No amyloid-β plaques or Lewy bodies were observed.

Discussion

BPAN is the first X-linked NBIA disorder to be described. Mutations in *WDR45* lead to a phenotype that is recognizable by its distinct pattern of clinical and radiographic features. During early childhood, subjects present with global developmental delay with slow language and motor gains until adolescence or early adulthood when dystonia, parkinsonism and cognitive decline become manifest. Comorbid features in childhood include seizures, spasticity, disordered sleep and stereotypies that further define the BPAN phenotype. Although, L-DOPA provides substantial initial benefit in BPAN, the benefit is short-lived and its use limited by dyskinesias. The prominent parkinsonism observed in BPAN justifies the designation of *WDR45* as a PARK family gene.

Consistent with these clinical features, the neuroimaging abnormalities found in BPAN indicate significant basal ganglia pathology. Iron accumulates earliest and to the highest levels in the substantia nigra and probably later and to a lesser extent in globus pallidus. In MRIs obtained very soon after deterioration (in adolescence), nigral iron is evident but the globus pallidus may not appear hypointense on T_2-weighted imaging, though pallidal iron is evident on GRE or T_2^* sequences (Fig. 1). Study subjects in the NBIA research registries were ascertained based on the presence of high iron in their brain on MRI or post-mortem examination. Therefore, the uniformity of this feature in the cohort presented may represent a bias of ascertainment.

A distinguishing and possibly unique feature of BPAN is the presence of a bright halo on T_1-weighted imaging in the substantia nigra and cerebral peduncles (Fig. 2). Hyperintense signal in this region seems to appear concomitantly with or soon after the clinical manifestations of dopaminergic loss. A possible explanation for this feature that is supported by the pathology results from one patient, is iron binding to neuromelanin, which is being released from dying pigmented neurons of the substantia nigra pars compacta (Faucheux *et al.*, 2003; Zhang *et al.*, 2011). Iron-neuromelanin complexes appear hyperintense on T_1 images; lipid can too (Enochs *et al.*, 1997; Faucheux *et al.*, 2003; Ginat and Meyers, 2012). Regardless, no other pathology leads to this specific 'halo' pattern in the substantia nigra on T_1 sequences.

A second imaging difference between BPAN and other forms of NBIA is the predominance of substantia nigra iron over that seen in the globus pallidus, especially early in disease. This pattern is also evident on gross and microscopic pathology. In two other forms of NBIA, phospholipase A_2-associated neurodegeneration (PLAN) and mitochondrial membrane protein-associated neurodegeneration (MPAN), iron accumulates more equally in these structures, and in pantothenate kinase-associated neurodegeneration it appears earliest and predominately in the globus pallidus (Fig. 4).

The pathology in BPAN distinguishes it from other NBIA disorders (Fig. 5). In BPAN, pathological changes in substantia nigra dominate those found in globus pallidus, whereas in pantothenate kinase-associated neurodegeneration the reverse is true. While Lewy body pathology is abundant in MPAN and PLAN, none is seen in BPAN. Thus, BPAN, like pantothenate kinase-associated neurodegeneration, is not a synucleinopathy (Kruer *et al.*, 2011). Finally, BPAN frequently manifests with atrophic changes in cerebellum, a feature shared with PLAN.

Although we recognized the BPAN phenotype more than a decade ago (Gregory and Hayflick, 2002; Gregory *et al.*, 2009), naming it in a manner consistent with terms used to designate other forms of NBIA had to await discovery of the causative gene. BPAN is the form of NBIA that is associated with mutations in *WDR45*. Though referenced in the literature, the term SENDA (static encephalopathy with neurodegeneration in adulthood) is no longer favoured (Gregory and Hayflick, 2011; Kruer *et al.*, 2012).

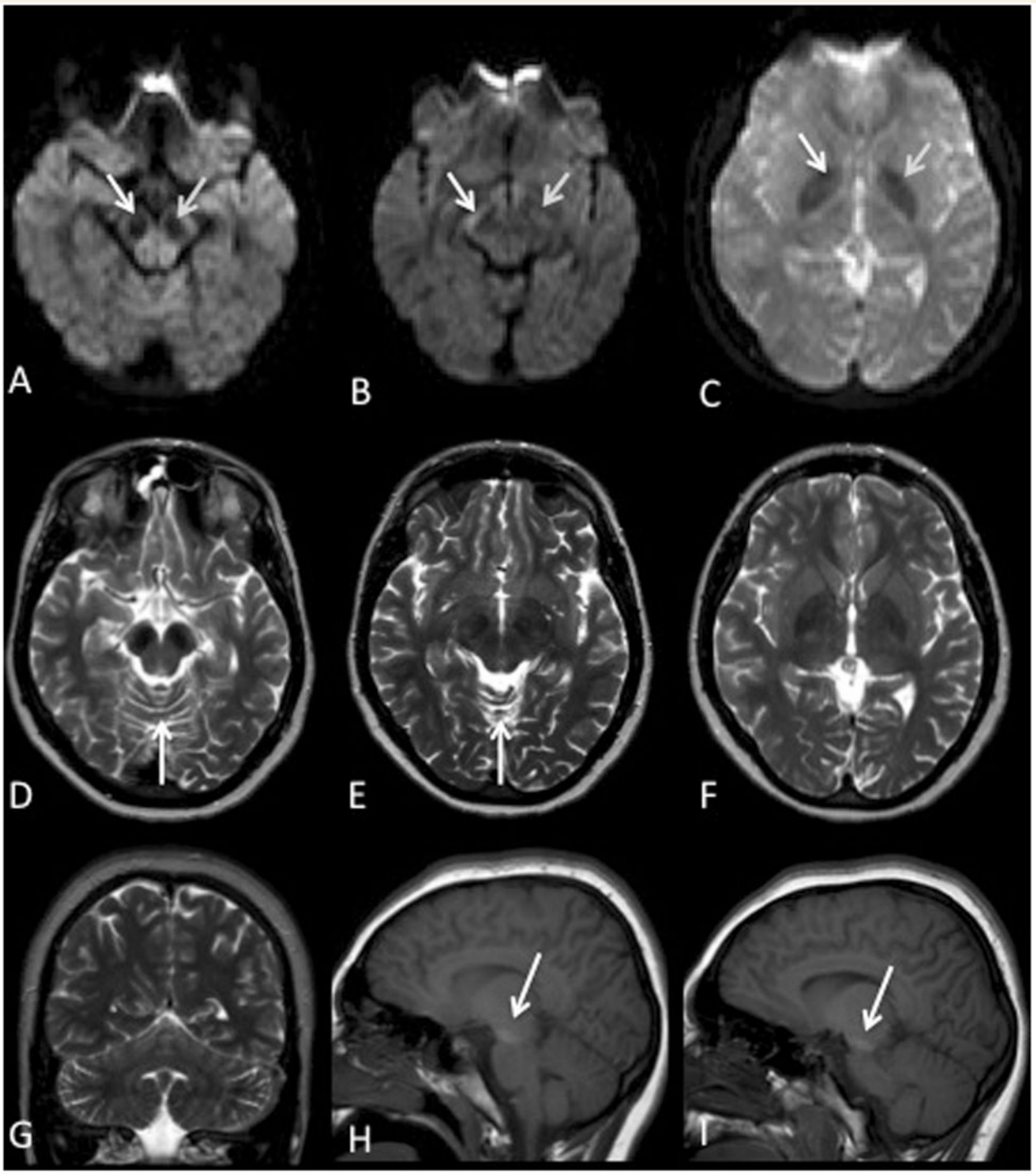

Figure 3 Early MRI features of BPAN. (**A**–**C**) Axial diffusion-weighted images acquired with an echo planar sequence through the midbrain, cerebral peduncles and basal ganglia shows marked hypointensity resulting from the iron deposition in (**A** and **B**) substantia nigra and (**C**) globus pallidi (arrows). (**D**–**F**) Corresponding T_2-weighted slices reveals hypointense signal in the corresponding regions as well as vermian atrophy (arrow). (**G**) Coronal T_2-weighted demonstrates more global cerebellar atrophy. (**H** and **I**) Sagittal images (*right* and *left*) show hyperintensity of the substantia nigra on T_1-weighted imaging within the midbrain and cerebral peduncles (arrows).

Consistent with the fact that *WDR45* is located on the X chromosome, there is a gender bias in our cohort. Most patients are female, supporting an X-linked dominant pattern of disease. Interestingly, three males demonstrate a phenotype that is indistinguishable from that of affected females. To date, all mutations are known or suspected to arise *de novo*, and males are predicted or known to harbour post-zygotic mutations to explain their viability (Haack *et al.*, 2012). Females may harbour either germline or somatic mutations to explain their disease. Similar patterns of disease have been documented in Rett syndrome, another X-linked

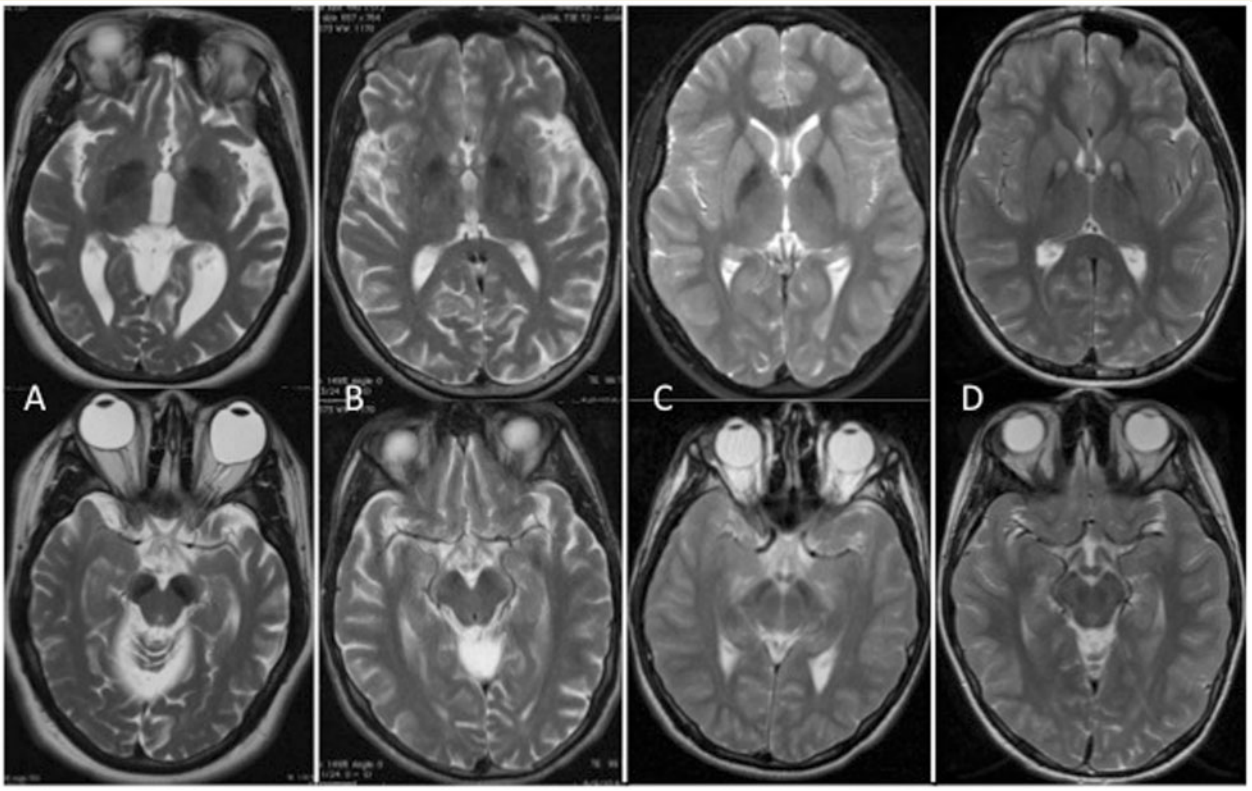

Figure 4 MRI of the globus pallidus and substantia nigra in four main forms of NBIA. Axial T_2-weighted imaging of globus pallidus (*top* series) and substantia nigra (*bottom* series) in (**A**) BPAN; (**B**) phospholipase A2-associated neurodegeneration; (**C**) mitochondrial membrane protein-associated neurodegeneration; and (**D**) pantothenate kinase-associated neurodegeneration.

dominant disorder. Moreover, we have implicated skewing of X chromosome inactivation as a factor influencing phenotypic manifestations in BPAN (Haack *et al.*, 2012).

In keeping with this interpretation of the genetic mechanism is the prediction that a much broader range of phenotypes will be found to be associated with mutations in *WDR45*. The timing during embryogenesis of somatic mutations will determine phenotypic severity. In males, this range is likely to span from severe neonatal encephalopathy to mild intellectual disability. It is likely that females would be 'protected' against a neonatal presentation of severe encephalopathy unless they lack a second X chromosome. Females harbouring relatively late somatic mutations or with a pattern of 'favourable' skewing of X chromosome inactivation are predicted to manifest a milder phenotype than that reported here. If their mutation is present in germ cells, then 50% of the female offspring of such females will have BPAN, and 50% of the male offspring probably will be non-viable. Although our study populations have been ascertained by the presence of high brain iron, we predict that patients without this feature but with neurodevelopmental abnormalities will be found with mutations in *WDR45*.

The *de novo* status of mutations in all families investigated explains why the reported patients are simplex cases. Moreover, it provides a basis for genetic counselling for recurrence risk, which is very low, although gonadal mosaicism remains a theoretical possibility. Parental testing for mutations in *WDR45* should be performed because very mildly affected individuals with a low level of somatic mosaicism or 'favourable' skewing of X chromosome inactivation may be at high risk for having a severely affected child. We found no evidence that increased maternal or paternal age is a risk factor, and have not yet established if there is a bias for mutations occurring on the maternally- versus paternally-derived X chromosome. Genetic testing of *WDR45* is now available in the clinical setting (www.genetests.org). Diagnostic testing of multiple tissues may be necessary in order to identify mutations in *WDR45* in those with somatic mosaicism.

With genetic testing, diagnosis of BPAN during childhood is now possible. BPAN should be suspected in a child with global developmental disabilities, especially if accompanied by seizures, disordered sleep or stereotypies. On brain MRI, we predict that T_1 hyperintense signal and T_2 hypointense signal in substantia nigra will be detectable by early in the second decade of life and possibly sooner, and this feature would justify clinical molecular testing for mutations in *WDR45*. Earlier detection will not only provide families with a diagnosis and accurate assessment of recurrence risk but may also enable appropriate therapeutic intervention for patients with subtle early symptoms of parkinsonism.

The clinical similarities between BPAN and atypical Rett syndrome are striking, and we propose that *WDR45* be added to the growing list of genes associated with a Rett-like phenotype. Both BPAN and atypical Rett syndrome cause neurodevelopmental regression with specific loss of limited expressive language skills. Two females with BPAN were described as having 'Rett-like

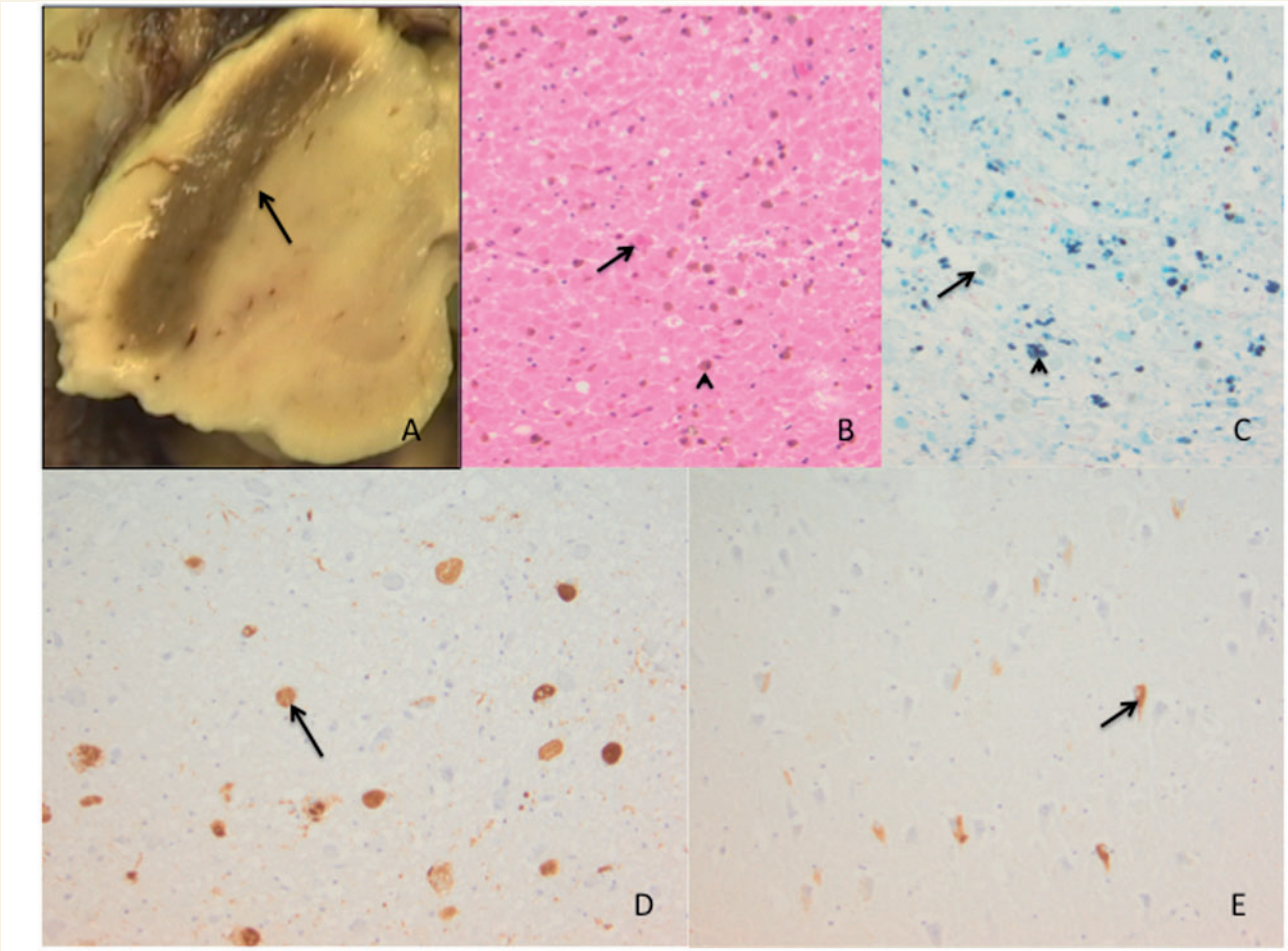

Figure 5 Pathological features of BPAN. The gross unstained substantia nigra demonstrating a homogenous grey/brown band (arrow) in (**A**); substantia nigra showing numerous large dystrophic axonal spheroids (arrow) and macrophages (arrowhead) full of haemosiderin (**B**, ×100, haematoxylin and eosin stain); same region with iron demonstrated by Prussian blue reaction (**C**, ×100); neurofibrillary tangles (arrows) in hypothalamus (**D**) the subiculum of the hippocampus (**E**, ×100, tau immunohistochemistry).

hand-wringing' and four more carried a suspected diagnosis of atypical Rett syndrome. In BPAN, intellectual disability followed by dementia in adulthood is reflected on the MRI as progressive cerebral volume loss, though unlike individuals with Rett syndrome, those with BPAN do not seem to acquire microcephaly. Seizures are common in both disorders, as are abnormal sleep patterns. The rare males with *MECP2* mutations can manifest parkinsonism, which is a key feature of BPAN. Both conditions are X-linked dominant, which is a conspicuously rare pattern of inheritance for a human disease. Testing for *WDR45* mutations should be considered in individuals with features of Rett syndrome who lack mutations in known Rett genes even without MRI evidence of high brain iron, especially in the paediatric age group. *WDR45* should be added to multi-gene panels for clinical molecular testing of Rett syndrome, variant Rett syndrome and X-linked intellectual disability. Testing of *WDR45* may also be indicated for individuals with an Angelman syndrome-like phenotype who lack a molecular abnormality involving 15q11.2-13. The prominence of seizures and of multiple seizure types in individuals with BPAN may justify the inclusion of *WDR45* in multigenic assays seeking a genetic basis for epileptic encephalopathies in childhood. Results of such testing will lead to new insights into the clinical spectrum of the BPAN phenotype in females as well as males.

A growing body of literature implicates dysregulation of autophagy as an important mechanism in the pathophysiology of neurodegeneration (Nassif and Hetz, 2012). In normal neurons, basal autophagy is important for protein quality control and organellar homeostasis. When cells are stressed or injured, the autophagic process is induced to clear damaged cellular components and by-products of the stress response. Defective autophagy would leave damaged cells compromised and at risk of perpetuating further damage to neighbouring cells. This cascade, when occurring in post-mitotic tissue such as brain, would present clinically with neurological deterioration after a threshold of cellular functional impairment is exceeded. Precisely how the beta-propeller protein that is encoded by *WDR45* serves the autophagic process remains to be elucidated. What is clear is that defects in this protein lead to a neurodevelopmental and neurodegenerative phenotype that is recognizable and able to be confirmed by molecular testing. As our clinical experience grows, understanding of the

pathophysiology of BPAN and ideas for rational therapeutics will follow. With autophagic dysregulation increasingly being implicated in Alzheimer disease, Huntington disease, and Parkinson disease (Nassif and Hetz, 2012), insights from this rare disorder are likely to advance understanding of more common disorders.

Acknowledgements

We gratefully acknowledge the support and participation worldwide of families with NBIA, who inspire us every day through their dedication and partnership via the NBIA Disorders Association, Hoffnungsbaum e.V., and Associazione Italiana Sindromi Neurodegenerative da Accumulo di Ferro. We thank Evelyn Botz and Carola Fischer for technical support, the Cell line and DNA bank of paediatric movement disorders of the Telethon Genetic Biobank Network (GTB07001), the UK Parkinson's Disease Consortium, UCL/Institute of Neurology, University of Sheffield and University of Dundee, the Medical Research Council, the Parkinson's Disease Foundation, the Dystonia Medical Research Foundation and the Brain Research Trust.

Funding

This work was supported by our advocacy partners: the NBIA Disorders Association; Hoffnungsbaum e.V.; and Associazione Italiana Sindromi Neurodegenerative da Accumulo di Ferro. This work was made possible with support from the Oregon Clinical and Translational Research Institute (UL1 RR024140 NCRR), a component of the NIH and NIH Roadmap for Medical Research. P.H., N.N., T.M., H.P. and S.J.H. participate in the TIRCON consortium (European Commission Seventh Framework Programme-FP7/2007-2013, HEALTH-F2-2011, Grant Agreement #277984). M.C.K. receives support from American Academy of Neurology, Dystonia Medical Research Foundation, Child Neurology Foundation and American Philosophical Society. M.A.K.'s research is supported by Great Ormond Street Children's Charities, Action Medical Research and the Wellcome Trust. T.M. and H.P. were supported by German Federal Ministry of Education and Research (BMBF)-funded Systems Biology of Metabotypes grant (SysMBo 0315494A) and German Network for Mitochondrial Disorders (mitoNET 01GM0867). T.M. was supported by European Commission 7th Framework Program (N. 261123), Genetic European Variation in Disease Consortium, and German Ministry for Education and Research (01GR0804-4).

References

Adzhubei IA, Schmidt S, Peshkin L, Ramensky VE, Gerasimova A, Bork P, et al. A method and server for predicting damaging missense mutations. Nat Methods 2010; 7: 248–9.

Behrends C, Sowa ME, Gygi SP, Harper JW. Network organization of the human autophagy system. Nature 2010; 466: 68–76.

Capriotti E, Casadio R. Predicting the insurgence of human genetic diseases associated to single point protein mutations with support vector machines and evolutionary information. Bioinformatics 2006; 22: 2729–34.

Egan RA, Weleber RG, Hogarth P, Gregory A, Coryell J, Westaway SK, et al. Neuro-ophthalmologic and electroretinographic findings in pantothenate kinase-associated neurodegeneration (formerly Hallervorden-Spatz syndrome). Am J Ophthalmol 2005; 140: 267–74.

Enochs WS, Petherick P, Bogdanova A, Mohr U, Weissleder R. Paramagnetic metal scavenging by melanin: MR imaging. Radiology 1997; 204: 417–23.

Faucheux BA, Martin ME, Beaumont C, Hauw JJ, Agid Y, Hirsch EC. Neuromelanin associated redox-active iron is increased in the substantia nigra of patients with Parkinson's disease. J Neurochem 2003; 86: 1142–8.

Ferrer-Costa C GJ, Zamakola L, Parraga I, de la Cruz X, Orozco M. PMUT: a web-based tool for the annotation of pathological mutations on proteins. Bioinformatics 2005; 21: 3176–8.

Ginat DT, Meyers SP. Intracranial lesions with high signal intensity on T1-weighted MR images: differential diagnosis. Radiographics 2012; 32: 499–516.

Gregory A, Hayflick SJ. Pantothenate Kinase-Associated Neurodegeneration. In *GeneReviews* at GeneTests Medical Genetics Information Resource (database online). Copyright, University of Washington, Seattle. 1997–2013. Available: http://www.genetests.org. (Jan 2013, date last accessed).

Gregory A, Hayflick SJ. Genetics of neurodegeneration with brain iron accumulation. Current neurology and neuroscience reports 2011; 11: 254–61.

Gregory A, Polster BJ, Hayflick SJ. Clinical and genetic delineation of neurodegeneration with brain iron accumulation. J Med Genet 2009; 46: 73–80.

Haack TB, Hogarth P, Kruer M, Gregory A, Wieland T, Schwarzmayr T, et al. Exome sequencing reveals de novo mutations in *WDR45* causing a phenotypically distinct, X-linked dominant form of NBIA. Am J Hum Genet 2012; 7: 11444–9.

Hogarth P, Gregory A, Kruer MC, Sanford L, Wagoner W, Natowicz M, et al. New NBIA subtype: genetic, clinical, pathologic, and radiographic features of MPAN. Neurology 2013; 80: 268–75.

Kruer MC, Boddaert N, Schneider SA, Houlden H, Bhatia KP, Gregory A, et al. Neuroimaging features of neurodegeneration with brain iron accumulation. AJNR Am J Neuroradiol 2012; 33: 407–14.

Kruer MC, Hiken M, Gregory A, Malandrini A, Clark D, Hogarth P, et al. Novel histopathologic findings in molecularly-confirmed pantothenate kinase-associated neurodegeneration. Brain 2011; 134 (Pt 4): 947–58.

Nassif M, Hetz C. Autophagy impairment: a crossroad between neurodegeneration and tauopathies. BMC Biol 2012; 10: 78.

Ng PC, Henikoff S. SIFT: predicting amino acid changes that affect protein function. Nucleic Acids Res 2003; 31: 3812–4.

Zhang W, Phillips K, Wielgus AR, Liu J, Albertini A, Zucca FA, et al. Neuromelanin activates microglia and induces degeneration of dopaminergic neurons: implications for progression of Parkinson's disease. Neurotox Res 2011; 19: 63–72.